A Retrospective Analysis of Remote-sensing Reflectance Products in Coastal and Inland Waters

Nima Pahlevan, Sundarabalan Balasubramanian, Christopher C. Begeman, Ryan E. O'Shea, Akash Ashapure, Daniel A. Maciel, Dorothy K. Hall, Daniel Odermatt, Claudia Giardino

***Abstract*— Constructing a robust ocean color (OC) record (e.g., water transparency, phytoplankton absorption) for long-term assessments of coastal and inland water ecosystems from past, present, and future missions requires high-quality spectral remote sensing reflectance (R_{rs}) products. Using the GLORIA dataset [1], we evaluated the quality of R_{rs} products from the Moderate Resolution Imaging Spectroradiometer (MODIS on Terra and Aqua), Medium Resolution Imaging Spectrometer (MERIS), and Visible Infrared Imaging Radiometer Suite (VIIRS) processed via the 2-band heritage atmospheric correction method (a combination of near-infrared and shortwave infrared bands) available in the SeaWiFS Analysis Data Analysis System (SeaDAS). Overall, retrieval residuals are consistent within a few percent among the four missions. Median residuals ranged from ~20% in the ~550 nm band to > 60% in the ~412 nm bands. Spectrally averaged root mean squared differences for all the missions were ~ 0.0024 sr^{-1} with one standard deviation of ~0.001 sr^{-1}. The corresponding (median) biases in the visible bands varied from -60 to -3%, with the largest biases identified in MERIS and VIIRS products. Despite the lower sensitivity of band-ratio algorithms to residuals in specific spectral regions (e.g., OC3 chlorophyll-a algorithm is less prone to residuals in $R_{rs}(\lambda > 600$ nm)), other algorithms or downstream products that leverage all the visible bands are highly compromised. We underscore the need to improve the quality of R_{rs} products, thereby enabling the reconstruction of baseline OC products of high caliber in global coastal and inland waters that are often near human activity.**

***Index Terms*— Ocean color, remote sensing reflectance, validation, coastal and inland waters, freshwater ecosystems, MODIS, MERIS, VIIRS.**

I. INTRODUCTION

Modern ocean color (OC) missions have long enabled assessments of the global ocean's properties for their biogeochemical variability, biomass, and organic contents from which nutrient availability and response to climate variability can be inferred [2]. While intended primarily for ocean studies, OC imagery and products have been broadly utilized in coastal estuaries and inland waters where societal impacts of climate variability and anthropogenic activities are most realized [3, 4]. As the Earth's biosphere and atmosphere continue to warm and extreme events bear on us more intensely and frequently, the value of historical OC products is (and will be) increasingly appreciated, as these products permit full comprehension of the amount and direction of trends in biogeochemical properties of water bodies on a global scale [5-8]. This is particularly crucial given the response time to climate variability, and because extreme events may vary in different aquatic ecosystems.

The concentration of chlorophyll-a (Chl*a*), the prime proxy for upper water-column phytoplankton biomass, is a widely used OC product for assessing changes in primary productivity, food availability, ecological seascapes, and algal bloom formation [9, 10]. Chl*a* algorithms of different constructs are employed depending on the water type, which is determined by the shape of the spectral water-leaving radiance or spectral remote sensing reflectance (R_{rs}) [11]. In blue waters (ocean, coastal shelves, oligotrophic lakes), the ratios of blue-green spectral bands are proven robust [12, 13], whereas, in productive inland waters, the red (665, 681 nm) and red-edge bands (709 nm) are conventionally applied in some forms of band-arithmetic calculation [14]. There is considerable variability in the reported residuals in Chl*a* products (20-70%) depending on the algorithm, use case, uncertainties in field measurements, and environmental conditions at the time of satellite overpass [15-23]. This range of inaccuracies results from a cascade of residuals in the respective R_{rs}, which are inherently reduced through band-arithmetic formulas. Despite its broad utility, Chl*a* is not the only quantity retrievable via OC observations. Spectral absorption and backscattering of phytoplankton, inorganic and organic particles, as well as dissolved matter, are used and studied in oceanic environments for multiple applications (e.g., computation of net primary production or carbon export [24, 25]. However, over coastal

This paragraph of the first footnote will contain the date on which you submitted your paper for review, which is populated by IEEE. This work was supported by NASA under grants 80NSSC22K1389 (RSWQ21) and 80NSSC22K0554 (TASNPP20), as well as SNSF scientific exchange grant number IZSEZ0_217542. *(Corresponding author:* Nima Pahlevan*;* nima.pahlevan@nasa.gov*).* Nima Pahlevan and Sundarabalan Balasubramanian contributed equally. Nima Pahlevan, Christopher Begeman (christopher.c.begeman@nasa.gov), Ryan O'Shea (ryan.e.o'shea@nasa.gov), and Akash Ashapure (akash.ashapure@nasa.gov) are with Science Systems and Applications Inc. (SSAI) and NASA Goddard Space Flight Center, Greenbelt, MD, 20771 USA. Sundarabalan Balasubramanian (vbsbalanin@gmail.com) was with the University of Maryland Baltimore County, Baltimore, MD 21228 USA, and is currently with Geosensing and Imaging Consultancy, Trivandrum, India. Daniel A. Maciel (daniel.maciel@inpe.br) is with the Earth Observation Coordination of the National Institute for Space Research (INPE), São José dos Campos/SP, 12227-010, Brazil. Dorothy Hall (dkhall1@umd.edu) is with the University of Maryland, College Park, MD 20740 USA. Daniel Odermatt (Daniel.Odermatt@eawag.ch) is with the Swiss Federal Institute of Aquatic Science and Technology, Dübendorf, 8600 Switzerland. Claudia Giardino (giardino.c@irea.cnr.it) is with the National Research Council of Italy, Milan 20133 Italy. Supplementary material, including several figures and tables, are provided in a separate file. Color versions of one or more figures in this article are available online at http://ieeexplore.ieee.org.

and inland waters, these spectral properties (referred to as the inherent optical properties; IOPs) from OC have been examined across limited spatiotemporal scales [26-29] due to significant residuals in R_{rs}, the lack of *in situ* validation data, or unfamiliarity of the user community with these products. Other water-color proxies, such as spectral diffuse attenuation coefficient (K_d) [30] or Secchi disk depth [31], which may require full spectral content within the visible spectrum, also suffer from high sensitivities to residuals in R_{rs}.

This study offers a retrospective analysis of R_{rs} products from the Moderate Resolution Imaging Spectroradiometer (MODIS), Medium Resolution Imaging Spectrometer (MERIS), and Visible Infrared Imaging Radiometer Suite (VIIRS) in coastal and inland waters using *in situ* radiometric data. For completeness, the satellite products were further paired and directly compared using the common matchups. Our chief objective is to warrant research directions for the improved quality of the OC archive, serving as a robust baseline for future multidecadal studies of coastal and inland waters.

II. Data and Methods

High-quality *in situ* radiometric data from the GLObal Reflectance community dataset for Imaging and optical sensing of Aquatic environments (GLORIA) [1] were resampled with the relative spectral response functions of the OC missions after the exclusion of the flagged data records. Satellite imagers included MODIS onboard Terra (MODIS/T) and Aqua (MODIS/A), European Space Agency's MERIS, and NASA/NOAA's VIIRS on Suomi-NPP (VIIRS/SNPP). See Table A1 in Supplementary Material for more information on the instruments and output grid cell size. The images were harmoniously processed to R_{rs} using an atmospheric correction approach suited for highly turbid and productive environments [32]. More specifically, while corrections for the effects of Rayleigh scattering and gaseous absorption were carried out similarly, we utilized the heritage two-band ratio scheme with varying band combinations for removing aerosol contributions (SeaDAS v8.2). These band combinations included 869 – 2130 nm for MODIS/T and MODIS/A, 779 – 865 nm for MERIS, and 862 – 2257 nm for VIIRS/SNPP. This strategy allowed for assessing the quality of R_{rs}(748), which carries information in highly turbid and eutrophic waters [33]. The rest of the input parameters, including sensor-specific vicarious calibration gains or cloud-masking thresholds, were set to default. We used NASA's processing method because, historically, it is the standard processing scheme for producing and archiving the OC record.

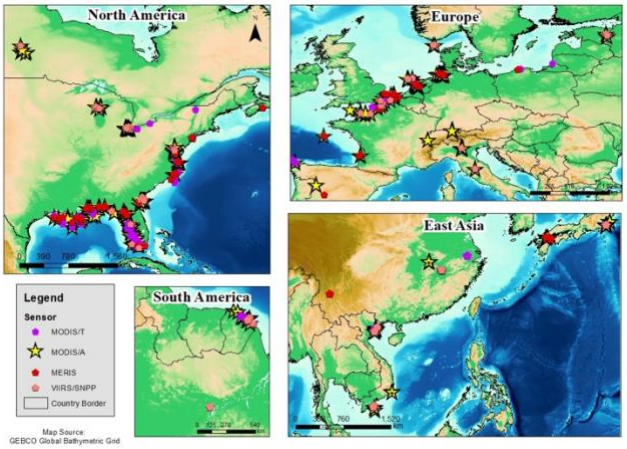

Fig. 1. Geographic representation of valid GLORIA [1] matchup dataset for the four sensors.

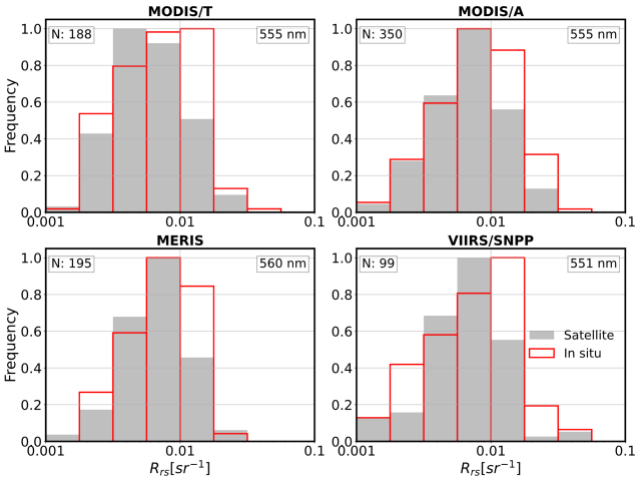

Fig. 2. Normalized frequency distributions of satellite and *in situ* R_{rs}(~550) for valid matchups of the four satellite missions.

The matchup identification and selection were conducted following widely accepted OC community procedures [34-36] (see Table A1). Matchups, extracted from 3×3-element kernels [37], were considered viable only if ≥ 6 pixels had valid R_{rs} retrievals and the coefficient of variation (CV defined as the ratio of standard deviation and mean) in the green band (e.g., 560 nm) was < 0.2 [38, 39]. The median operator was applied to compute satellite-derived R_{rs} for a matchup acquired within the +/-3 hours span of satellite overpasses, although time differences of +/-6 hours were also investigated for completeness (e.g., Fig. A7). To eliminate invalid matchups in extreme aquatic conditions (e.g., highly turbid or organic-rich waters [40]), data points with R_{rs}(~667) > 0.012 sr^{-1}, R_{rs}(~667) < 0.10^{-4} sr^{-1}, and R_{rs}(~412) < 0 sr^{-1} were discarded. For cross-mission comparisons of common matchups (**Fig. 5**), time-difference constraints were not applicable as the morning (MODIS/T and MERIS) and afternoon (MODIS/A and VIIRS/SNPP) missions follow one another within an hour. Further, we employed a cubic polynomial fit to account for the differences in the spectral bands [41] and increased the MERIS and VIIRS/SNPP matchup kernel sizes to closely match that of MODIS (e.g., a 10×10-element window for MERIS).

For the statistical assessments, we used a wide range of conventional linear and log-based metrics (see Supplementary Material) to permit comparisons with previous reports while considering the log distribution of the matchup data [42]. These metrics include log-transformed metrics, such as the median symmetric residuals (MdSR; ε), signed symmetric bias parameter (SSBP; β), mean symmetric residual (MSR), root mean squared (log) difference (RMSLD), mean absolute (log)

residual (MAR), as well as mean bias (BIAS), root mean squared difference (RMSD), and the slope of linear regression computed in the linear space. The Pearson correlation coefficient (r) is also presented for the cross-mission analyses.

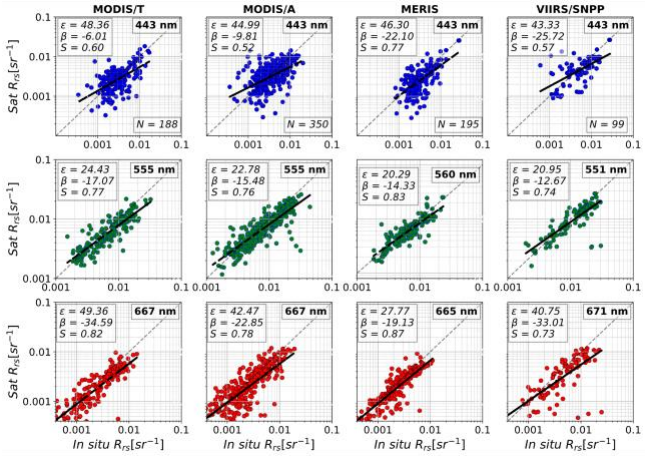

Fig. 3. Quality assessment of R_{rs} products in select bands from MODIS/T, MODIS/A, MERIS, and VIIRS/SNPP. Median residuals (ε), median bias (β), the slope of the linear regression (S), and the numbers of matchups are annotated. See Supplementary Material for more results.

III. Results

The global distribution and frequency distribution of valid satellite and *in situ* R_{rs} matchups (N ~ 550) are shown in **Figs. 1** and **2**, respectively (see Table A2 for the effects of different exclusion criteria on the number of matchups). The average of *in situ* data histograms are centered around 0.01 sr^{-1} (in log scale), which is nearly twice larger than those reported in previous AERONET-OC-centered validation exercises [43]. Scatterplots depicting the quality of satellite-derived products in select bands (443, 555, and 667 nm) are shown in **Fig. 3**. The median residuals (ε) for the four instruments are 43-48%, 20-24%, and 27-49% in the 443, ~555, and ~667 nm bands, respectively. Although the number of matchups differs from 99 to 350 for all the missions, the statistics vary only slightly, particularly in the 443 nm band. The biases (β) point to underestimations throughout all the visible bands (see Tables A3 through A6), from 7 to 61% in the blue, 7-20% in the green, and 17-36% in the red bands. In general, VIIRS products contain the highest negative biases. The slopes of the linear regression further indicate skewed distributions around the 1:1 line with overestimations at low signal levels and underestimations at increased R_{rs} magnitudes (e.g., > 0.01 sr^{-1} in the green bands). A broader set of metrics for six visible-near-infrared (VNIR) bands is depicted in **Fig. 4.**

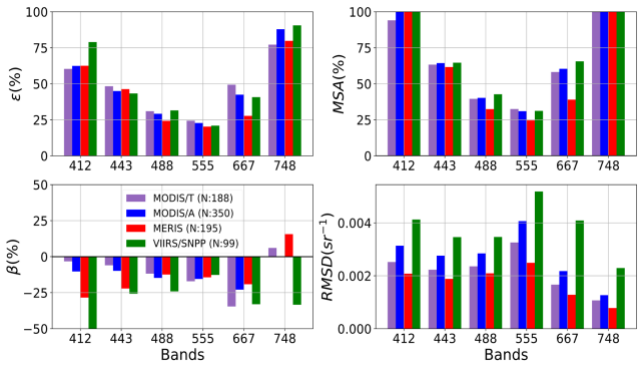

Fig. 4. Bulk statistical descriptors for R_{rs} products from MODIS/T, MODIS/A, MERIS, and VIIRS/SNPP. See Supplementary Material for the definition of the metrics and other performance measures in other spectral bands.

Direct intercomparisons of R_{rs} products for each mission pair are shown in **Fig. 5**. The most significant departure from the 1:1 line is in the 412, 443, and ~748 nm bands for which MERIS and VIIRS/SNPP products exhibit lower magnitudes than those of MODIS. While the red bands are consistent in the 0.001 – 0.01 sr^{-1} range, the corresponding agreements diminish for R_{rs} < 0.001 sr^{-1}, a range often encountered in moderately turbid coastal waters. The R_{rs} products are consistent across the entire dynamic range in the ~ 555 nm bands. See Table A7 for detailed statistical metrics. The cross-mission analysis in terms of R_{rs} residuals [43] (e.g., $\Delta R_{rs} = R_{rs}^{MODIS/A} - R_{rs}^{in\ situ}$) for MODIS/A & VIIRS/SNPP is illustrated in **Fig. 6**. With an identical processing scheme, one would expect the residuals to be highly correlated. This is true for the MODIS/A and VIIRS/SNPP products with r ≥ 0.8, whereas for MODIS/T and MERIS, the correlation coefficient exceeds 0.8 only in the green and NIR bands (see Fig. A5). This poorer agreement is likely attributed to MODIS/T calibration issues [44].

IV. Discussion

This brief study reinforces the presence of significant residuals in SeaDAS-processed R_{rs} products from heritage OC missions in typically turbid and eutrophic coastal and inland waters. The spectral behavior of residuals conforms to the established knowledge from AERONET-OC matchup analyses [34, 40, 43, 45]. Nevertheless, we demonstrated sizeable residuals (e.g., median or mean differences, biases) across all relevant VNIR bands, with VIIRS-derived products showing the largest residuals, particularly in the blue and red bands (**Fig. 4**). This is followed by MERIS and MODIS/T R_{rs} products, which have the second and third largest biases in all the bands,

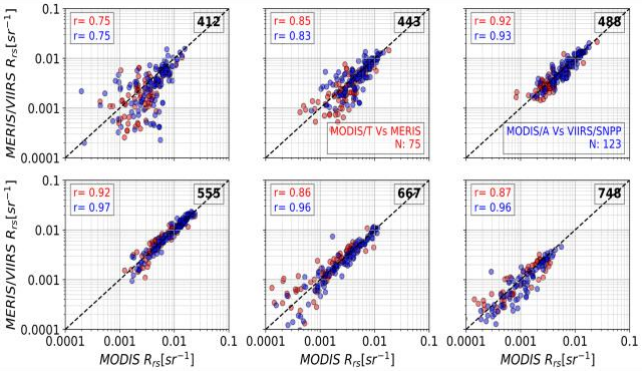

Fig. 5. Direct intercomparison of R_{rs} products for same-day, common GLORIA matchups of MERIS – MODIS/T (red circles) and VIIRS/SNPP – MODIS/A (blue circles). MODIS Terra or Aqua products are shown on the x-axes.

even though the median- and mean-residual metrics signify similar (but slightly larger) inaccuracies in MODIS/A products (**Fig. 4**). One should, however, note that we did not take into account failure in retrievals (e.g., $R_{rs}(412) < 0$ sr^{-1}) encountered in organic/sediment-rich waters [46]. For the OC missions, uncertainties due to adjacency effects (AE) from land and clouds are of greater concern compared to other factors, such as skyglint [47] or the black-pixel assumption violation [48]. To evaluate the presence of AE, we plotted the residuals as a function of distance from the shoreline (see Figs. A6 and A7) and found moderate correlations. This moderate correspondence is likely due to dependencies on other parameters, such as solar zenith angles, viewing zenith angles, and aerosol optical properties [43]. Further, an optical-water-type (OWT) analysis (see Fig. A8) revealed more significant residuals in eutrophic waters of types 4 and 5, defined in [42].

It is well recognized that Chl*a* or other empirical or semi-analytical schemes (e.g., the ocean-color-3 scheme (OC3) often uses ~488/551 nm low-residual bands) that are solely dependent on two or three bands may still offer fit-for-purpose products (e.g., mapping relative spatial variability in biomass). For example, OC-3 is known to overestimate Chl*a* due to underestimated satellite-derived R_{rs} [49, 50]. Our results ($\varepsilon >$ 20%) suggest that inversion techniques or downstream products (e.g., K_d) that rely on the magnitude of R_{rs} in one or all the visible bands would be heavily susceptible to these large residuals. For instance, phytoplankton or non-algal particle absorption spectra will likely carry significant residuals, constraining their use for tracking ecosystem responses to climate variability or long-term assessments of how the carbon cycle in coastal and inland regions fluctuate [51]. Hence, it is imperative that these invaluable multi-decadal products that form the basis of long-term spatiotemporal assessments in coastal and inland waters be revised and enhanced. Looking ahead, current (e.g., Sentinel-3's Ocean and Land Color Instrument) and upcoming satellite missions with improved spectral capability will require drastically enhanced R_{rs} products in the VNIR region to enable advancing and broadening the utility of OC observations beyond mere Chl*a* products (e.g., phytoplankton types).

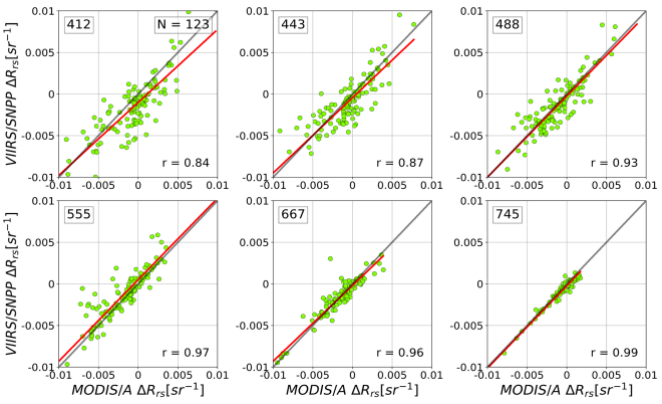

Fig. 6. Intercomparison of R_{rs} residuals (e.g., $\Delta R_{rs} = R_{rs}^{MODIS/A} - R_{rs}^{in\ situ}$) for same-day, common GLORIA matchups for VIIRS/SNPP and MODIS/A.

V. Conclusion

Using a recently published *in situ* R_{rs} dataset representing coastal and inland waters, we quantified the bulk residuals in MODIS-, MERIS-, and VIIRS-derived R_{rs} products to underscore the need for refined atmospheric correction mechanisms, enabling the establishment of robust OC records in the vicinity of human settlements. With negative biases within 3 – 60%, this study complements previous validation studies and further reinforces the need to improve the quality of R_{rs} products central to the viability of downstream products (beyond Chl*a*) in optically complex waters. Future endeavors will enhance and widen the utility of the invaluable OC archive in preparation for advanced missions, such as the Plankton, Aerosol, Cloud, ocean Ecosystem (PACE).

Acknowledgment

NASA's Ocean Biology Processing Group (OBPG) at Goddard Space Flight Center is acknowledged for the archival, maintenance, and improvement of the global OC record.

References

[1] M. K. Lehmann *et al.*, "GLORIA - A globally representative hyperspectral in situ dataset for optical sensing of water quality," *Scientific Data*, vol. 10, no. 1, p. 100, 2023/02/16 2023, doi: 10.1038/s41597-023-01973-y.

[2] B. Franz, M. Behrenfeld, D. Siegel, and P. Werdell, "Global ocean phytoplankton [in State of the Climate in 2013]," *Bull. Amer. Meteor. Soc*, vol. 95, no. 7, pp. S78-S80, 2014.

[3] R. L. Miller and B. A. McKee, "Using MODIS Terra 250 m imagery to map concentrations of total suspended matter in coastal waters," *Remote sensing of Environment*, vol. 93, no. 1, pp. 259-266, 2004.

[4] J. F. Gower, L. Brown, and G. Borstad, "Observation of chlorophyll fluorescence in west coast waters of Canada using the MODIS satellite sensor," *Canadian Journal of Remote Sensing*, vol. 30, no. 1, pp. 17-25, 2004.

[5] T. L. Frölicher, E. M. Fischer, and N. Gruber, "Marine heatwaves under global warming," *Nature*, vol. 560, no. 7718, pp. 360-364, 2018/08/01 2018, doi: 10.1038/s41586-018-0383-9.

[6] Z. Cao, H. Duan, L. Feng, R. Ma, and K. Xue, "Climate- and human-induced changes in suspended particulate matter over Lake Hongze on short and long timescales," *Remote Sensing of Environment*, vol. 192, pp. 98-113, 2017/04/01/ 2017, doi: 10.1016/j.rse.2017.02.007.

[7] S. Sathyendranath, R. J. Brewin, T. Jackson, F. Mélin, and T. Platt, "Ocean-colour products for climate-change studies: What are their ideal characteristics?," *Remote Sensing of Environment*, vol. 203, pp. 125-138, 2017.

[8] A. M. Michalak, "Study role of climate change in extreme threats to water quality," *Nature*, vol. 535, no. 7612, pp. 349-350, 2016.

[9] H. R. Gordon, D. K. Clark, J. W. Brown, O. B. Brown, R. H. Evans, and W. W. Broenkow, "Phytoplankton pigment concentrations in the Middle Atlantic Bight: comparison of ship determinations and CZCS estimates," *Appl. Optics*, vol. 22, no. 1, pp. 20-36, 1983/01/01 1983, doi: 10.1364/AO.22.000020.

[10] S. Son, T. Platt, H. Bouman, D. Lee, and S. Sathyendranath, "Satellite observation of chlorophyll and nutrients increase induced by Typhoon Megi in the Japan/East Sea," *Geophysical research letters*, vol. 33, no. 5, 2006.

[11] T. S. Moore, J. W. Campbell, and H. Feng, "A fuzzy logic classification scheme for selecting and blending satellite ocean color algorithms," *Geoscience and Remote Sensing, IEEE Transactions on*, vol. 39, no. 8, pp. 1764-1776, 2001.

[12] J. E. O'Reilly and P. J. Werdell, "Chlorophyll algorithms for ocean color sensors-OC4, OC5 & OC6," *Remote sensing of environment*, vol. 229, pp. 32-47, 2019.

[13] J. E. O'Reilly *et al.*, "Ocean color chlorophyll algorithms for SeaWiFS," *Journal of Geophysical Research: Oceans*, vol. 103, no. C11, pp. 24937-24953, 1998.

[14] W. J. Moses, A. A. Gitelson, S. Berdnikov, and V. Povazhnyy, "Satellite estimation of chlorophyll-a concentration using the red and NIR bands of MERISThe azov sea case study," *IEEE Geoscience and Remote Sensing Letters*, vol. 6, no. 4, pp. 845-849, 2009.

[15] S. Shang, Q. Dong, C. M. Hu, G. Lin, Y. Li, and S. Shang, "On the consistency of MODIS chlorophyll $ a $ products in the northern South China Sea," *Biogeosciences*, vol. 11, p. 269, 2014.

[16] M. Kahru, R. Kudela, C. Anderson, M. Manzano-Sarabia, and B. Mitchell, "Evaluation of satellite retrievals of ocean chlorophyll-a in the California Current," *Remote Sensing*, vol. 6, no. 9, pp. 8524-8540, 2014.

[17] J. N. Waite and F. J. Mueter, "Spatial and temporal variability of chlorophyll-a concentrations in the coastal Gulf of Alaska, 1998–2011, using cloud-free reconstructions of SeaWiFS and MODIS-Aqua data," *Progress in Oceanography*, vol. 116, pp. 179-192, 2013.

[18] C. Le *et al.*, "Towards a long-term chlorophyll-a data record in a turbid estuary using MODIS observations," *Progress in Oceanography*, vol. 109, pp. 90-103, 2013.

[19] G. H. Tilstone *et al.*, "Assessment of MODIS-Aqua chlorophyll-a algorithms in coastal and shelf waters of the eastern Arabian Sea," *Continental Shelf Research*, vol. 65, pp. 14-26, 2013.

[20] C. Hu, Z. Lee, and B. Franz, "Chlorophylla algorithms for oligotrophic oceans: A novel approach based on three-band reflectance difference," *Journal of Geophysical Research: Oceans*, vol. 117, no. C1, 2012.

[21] W. J. Moses *et al.*, "Estimation of chlorophyll-a concentration in turbid productive waters using airborne hyperspectral data," *Water research*, vol. 46, no. 4, pp. 993-1004, 2012.

[22] Y. Zhang, H. Lin, C. Chen, L. Chen, B. Zhang, and A. A. Gitelson, "Estimation of chlorophyll-a concentration in estuarine waters: case study of the Pearl River estuary, South China Sea," *Environmental Research Letters*, vol. 6, no. 2, p. 024016, 2011.

[23] H. M. Dierssen, "Perspectives on empirical approaches for ocean color remote sensing of chlorophyll in a changing climate," *Proceedings of the National Academy of Sciences*, vol. 107, no. 40, pp. 17073-17078, 2010.

[24] T. Smyth, G. Tilstone, and S. Groom, "Integration of radiative transfer into satellite models of ocean primary production," *Journal of Geophysical Research: Oceans*, vol. 110, no. C10, 2005.

[25] M. J. Behrenfeld, E. Boss, D. A. Siegel, and D. M. Shea, "Carbon-based ocean productivity and phytoplankton physiology from space," *Global biogeochemical cycles*, vol. 19, no. 1, 2005.

[26] Y. Qin, V. E. Brando, A. G. Dekker, and D. Blondeau-Patissier, "Validity of SeaDAS water constituents retrieval algorithms in Australian tropical coastal waters," *Geophysical Research Letters*, vol. 34, no. 21, 2007, doi: 10.1029/2007gl030599.

[27] L. Li *et al.*, "An inversion model for deriving inherent optical properties of inland waters: Establishment, validation and application," *Remote Sensing of Environment*, vol. 135, pp. 150-166, 2013/08/01/ 2013, doi: 10.1016/j.rse.2013.03.031.

[28] C. B. Mouw *et al.*, "Evaluation and optimization of bio-optical inversion algorithms for remote sensing of Lake Superior's optical properties," *Journal of Geophysical Research: Oceans*, vol. 118, no. 4, pp. 1696-1714, 2013.

[29] D. Odermatt, A. Gitelson, V. E. Brando, and M. Schaepman, "Review of constituent retrieval in optically deep and complex waters from satellite imagery," *Remote sensing of environment*, vol. 118, pp. 116-126, 2012.

[30] M. Wang, S. Son, and L. W. Harding Jr, "Retrieval of diffuse attenuation coefficient in the Chesapeake Bay and turbid ocean regions for satellite ocean color applications," *Journal of Geophysical Research: Oceans*, vol. 114, no. C10, 2009.

[31] J. Pitarch and Q. Vanhellemont, "The QAA-RGB: A universal three-band absorption and backscattering retrieval algorithm for high resolution satellite sensors. Development and implementation in ACOLITE," *Remote Sensing of Environment*, vol. 265, p. 112667, 2021.

[32] D. Aurin, A. Mannino, and B. Franz, "Spatially resolving ocean color and sediment dispersion in river plumes, coastal systems, and continental shelf waters," *Remote Sensing of Environment*, vol. 137, pp. 212-225, 2013.

[33] T. Wynne, R. Stumpf, and T. Briggs, "Comparing MODIS and MERIS spectral shapes for cyanobacterial bloom detection," *International journal of remote sensing*, vol. 34, no. 19, pp. 6668-6678, 2013.

[34] B. B. Barnes, J. P. Cannizzaro, D. C. English, and C. Hu, "Validation of VIIRS and MODIS reflectance data in coastal and oceanic waters: An assessment of methods," *Remote Sensing of Environment*, vol. 220, pp. 110-123, 2019.

[35] S. W. Bailey and P. J. Werdell, "A multi-sensor approach for the on-orbit validation of ocean color satellite data products," *Remote Sensing of Environment*, vol. 102, no. 1–2, pp. 12-23, 5/30/ 2006, doi: http://dx.doi.org/10.1016/j.rse.2006.01.015.

[36] J. A. Concha, M. Bracaglia, and V. E. Brando, "Assessing the influence of different validation protocols on Ocean Colour match-up analyses," *Remote Sensing of Environment*, vol. 259, p. 112415, 2021.

[37] V. E. Brando, J. L. Lovell, E. A. King, D. Boadle, R. Scott, and T. Schroeder, "The potential of autonomous ship-borne hyperspectral radiometers for the validation of ocean color radiometry data," *Remote Sensing*, vol. 8, no. 2, p. 150, 2016.

[38] G. Zibordi, J.-F. Berthon, F. Mélin, D. D'Alimonte, and S. Kaitala, "Validation of satellite ocean color primary products at optically complex coastal sites: Northern Adriatic Sea, Northern Baltic Proper and Gulf of Finland," *Remote Sensing of Environment*, vol. 113, no. 12, pp. 2574-2591, 2009.

[39] S. Hlaing *et al.*, "Evaluation of the VIIRS ocean color monitoring performance in coastal regions," *Remote sensing of environment*, vol. 139, pp. 398-414, 2013.

[40] C. Goyens, C. Jamet, and T. Schroeder, "Evaluation of four atmospheric correction algorithms for MODIS-Aqua images over contrasted coastal waters," *Remote Sensing of Environment*, vol. 131, pp. 63-75, 2013.

[41] S. I. Salem, H. Higa, J. Ishizaka, N. Pahlevan, and K. Oki, "Spectral band-shifting of multispectral remote-sensing reflectance products: Insights for matchup and cross-mission consistency assessments," *Remote Sensing of Environment*, vol. 299, p. 113846, 2023/12/15/ 2023, doi: https://doi.org/10.1016/j.rse.2023.113846.

[42] N. Pahlevan *et al.*, "ACIX-Aqua: A global assessment of atmospheric correction methods for Landsat-8 and Sentinel-2 over lakes, rivers, and coastal waters," *Remote Sensing of Environment*, vol. 258, p. 112366, 2021/06/01/ 2021, doi: https://doi.org/10.1016/j.rse.2021.112366.

[43] F. Mélin, "Validation of ocean color remote sensing reflectance data: Analysis of results at European coastal sites," *Remote Sensing of Environment*, vol. 280, p. 113153, 2022.

[44] B. A. Franz, E. J. Kwiatkowska, G. Meister, and C. R. McClain, "Utility of MODIS-Terra for ocean color applications - art. no. 66770Q," in *Earth Observing Systems Xii*, vol. 6677, J. J. Butler and J. Xiong Eds., (Proceedings of the Society of Photo-Optical Instrumentation Engineers (Spie), 2007, pp. Q6770-Q6770.

[45] G. Zibordi, F. Mélin, J.-F. Berthon, and E. Canuti, "Assessment of MERIS ocean color data products for European seas," *Ocean Science*, vol. 9, no. 3, pp. 521-533, 2013.

[46] M. Wang, S. Son, and W. Shi, "Evaluation of MODIS SWIR and NIR-SWIR atmospheric correction algorithms using SeaBASS data," *Remote Sensing of Environment*, vol. 113, no. 3, pp. 635-644, 2009.

[47] A. Gilerson, C. Carrizo, R. Foster, and T. Harmel, "Variability of the reflectance coefficient of skylight from the ocean surface and its implications to ocean color," *Optics express*, vol. 26, no. 8, pp. 9615-9633, 2018.

[48] D. A. Siegel, M. Wang, S. Maritorena, and W. Robinson, "Atmospheric correction of satellite ocean color imagery: the black pixel assumption," *Appl. Optics*, vol. 39, no. 21, pp. 3582-3591, 2000.

[49] P. J. Werdell, S. W. Bailey, B. A. Franz, L. W. Harding Jr, G. C. Feldman, and C. R. McClain, "Regional and seasonal variability of chlorophyll-a in Chesapeake Bay as observed by SeaWiFS and MODIS-Aqua," *Remote Sensing of Environment*, vol. 113, no. 6, pp. 1319-1330, 2009.

[50] F. H. Freitas and H. M. Dierssen, "Evaluating the seasonal and decadal performance of red band difference algorithms for chlorophyll in an optically complex estuary with winter and summer blooms," *Remote Sensing of Environment*, vol. 231, p. 111228, 2019.

[51] F. Cao *et al.*, "Remote sensing retrievals of colored dissolved organic matter and dissolved organic carbon dynamics in North American estuaries and their margins," *Remote Sensing of Environment*, vol. 205, pp. 151-165, 2018.